Warm asymmetric nuclear matter and proto-neutron star structure

Pravat Kumar Jena* and Lambodar Prasad Singh†
Department of Physics, Utkal University, Vanivihar, Bhubaneswar-751004, India
(Received 2 October 2003; published 20 October 2004)

The asymmetric nuclear matter equation of state at finite temperature is studied in the SU(2) chiral sigma model using mean-field approximation. The effect of temperature on effective mass, entropy, and binding energy is discussed. Treating the system to possess two conserved charges, the liquid-gas phase transition is investigated. We have also discussed the effect of the proton fraction on critical temperature with and without a ρ-meson contribution. We also apply our model to study the structure of the proto-neutron star with neutrino free charge-neutral matter in beta equilibrium. We found that the mass and radius of the star decreases as it cools from the entropy per baryon $S=2$ to $S=0$ and the maximum temperature of the core of the star is about 62 MeV for $S=2$.

DOI: 10.1103/PhysRevC.70.045803 PACS number(s): 26.60.+c, 21.30.Fe, 21.60.Jz

I. INTRODUCTION

A precise knowledge of the properties of nuclear matter at normal nuclear density and higher is of great importance for the understanding of compact stellar objects like neutron stars and the results of heavy-ion collision experiments. One of the celebrated models for study of nuclear matter using a relativistic quantum mean field was introduced by Walecka [1] involving a scalar and a vector field along with the nucleon field. This model and its extensions [2], while reproducing familiar nuclear properties well, gives rather a high value for the nuclear bulk modulus. A parallel and equally powerful model to study nuclear matter has been to use the chiral symmetry first emphasized by Lee and Wick [3]. The nonlinear terms in the chiral sigma model give rise to the three-body forces which become significant in the high density regime [4]. Further, the energy per nucleon at saturation needed the introduction of a dynamically generated isoscalar field [5] in addition to the scalar field of pions [6]. The incorporation of the interaction of the isospin triplet ρ-vector meson has been found essential for description of neutron-rich asymmetric nuclear matter [7]. The modified SU(2) chiral sigma model (MCH) with the introduction of cubic and quartic interaction terms [8] have been used by us in our earlier works [9] to study the phase transition between quark and nuclear matter and the structure of a hybrid star with one and two conserved charges at zero temperature. However, since the description of astrophysical and heavy-ion collision phenomena requires the study of asymmetric nuclear matter at finite temperature, we, in this work wish to extend our modified SU(2) chiral sigma model approach to finite temperatures.

The study of properties of hot dense asymmetric nuclear matter has been, in the last few years, vigorously pursued in connection with astrophysical problems [10,11], such as supernova explosions, the evolution of neutron stars, and heavy-ion collisions. As the equation of state (EOS) describes the variation of energy density and pressure with density and temperature, it can be used to study gaseous and liquid nuclear matter phases up to the deconfinement transition. It is also possible to study the liquid-gas phase transition, which may occur in the warm and dilute nuclear matter produced in heavy-ion collisions. Several authors using nonrelativistic [12] and relativistic [13–17] theories have studied liquid-gas phase transition. Most of the calculations found the critical temperature T_c lying in the range of 14–20 MeV for symmetric nuclear matter. The critical temperature of symmetric nuclear matter for the relativistic Walecka model is $T_c \approx 18.3$ MeV [18]. As the asymmetry parameter or the proton fraction plays a vital role in determining the critical temperature, the addition of a ρ meson is quite essential for the study of asymmetric nuclear matter [13,14].

Field theoretical finite temperature EOS plays an important role in studying the properties and structure of hot dense massive stars such as proto-neutron stars at different temperatures and densities. The important characteristics which determine the composition of matter in a compact star are [19] their relative compressibilities (important to determine the maximum mass of neutron star), symmetry energies (important to determine the typical stellar radius and the relative n, p, e, neutrino abundances), and specific heats (important to determine local temperatures). These characteristics vary with the EOS used in different models. Generally, the structures of both hot and cold, and both neutron-rich and neutron-poor, stars are fixed by the EOS [11]. A proto-neutron star [PNS] is born following the gravitational collapse of the core of a massive star during a supernova explosion (type II) and evolves to a cold and deleptonized neutron star, basically through neutrino emission. This very dense and hot core is also able to trap neutrinos, imparting momentum to the outer layers and then cooling as it reaches a quasiequilibrium state. There can also be a quark-hadron phase transition in PNS at high density and temperature [20].

In this paper we have extended our earlier study [21] on finite temperature EOS by adding a ρ meson to the Lagrangian density within the MCH model [9] as the addition of the ρ meson is quite essential for the study of asymmetric nuclear matter. In our earlier work we have studied the effect of temperature on EOS, effective mass, entropy, and binding

*Email address: pkjena@iopb.res.in
†Email address: lambodar@iopb.res.in

energy for symmetric nuclear matter and investigated the liquid-gas phase transition using the same model without the ρ meson. We now study here how the asymmetry parameter or proton fraction in addition to the ρ meson changes those properties at finite temperatures. As finite temperature EOS has an important role in studying the structure and properties of astrophysical objects, we have also investigated the structure of PNS taking β-stable charge neutral matter without neutrinos consisting of neutrons, protons, and electrons only.

In Sec. II, application of our model to the study of asymmetric nuclear matter at finite temperature is presented. In Sec. III, we apply our model to study the characteristics of the proto-neutron star. We conclude with some remarks in Sec. IV.

II. ASYMMETRIC NUCLEAR MATTER AT FINITE TEMPERATURE

A. Equation of state

Continuing our earlier investigation [9] on the study of the finite temperature effect of asymmetric nuclear matter using the MCH model, we include here the ρ field in the Lagrangian density. The EOS for the hadronic phase is calculated by using the Lagrangian density [13] (with $\hbar=c=K_{\text{Boltzmann}}=1$),

$$\begin{aligned} L = {} & \frac{1}{2}(\partial_\mu\vec{\pi}\cdot\partial^\mu\vec{\pi}+\partial_\mu\sigma\partial^\mu\sigma)-\frac{1}{4}F_{\mu\nu}F^{\mu\nu}-\frac{\lambda}{4}(x^2-x_0^2)^2 \\ & -\frac{\lambda B}{6m^2}(x^2-x_0^2)^3-\frac{\lambda C}{8m^4}(x^2-x_0^2)^4-g_\sigma\bar{\psi}(\sigma+i\gamma_5\vec{\tau}\cdot\vec{\pi})\psi \\ & +\bar{\psi}(i\gamma_\mu\partial^\mu-g_\omega\gamma_\mu\omega^\mu)\psi+\frac{1}{2}g_\omega^2x^2\omega_\mu\omega^\mu-\frac{1}{4}G_{\mu\nu}G^{\mu\nu} \\ & +\frac{1}{2}m_\rho^2\vec{\rho}_\mu\cdot\vec{\rho}^\mu-\frac{1}{2}g_\rho\bar{\psi}(\vec{\rho}_\mu\cdot\vec{\tau}\gamma^\mu)\psi. \end{aligned} \tag{1}$$

In the above Lagrangian, $F_{\mu\nu}\equiv\partial_\mu\omega_\nu-\partial_\nu\omega_\mu, G_{\mu\nu}\equiv\partial_\mu\rho_\nu-\partial_\nu\rho_\mu$, and $x=(\vec{\pi}^2+\sigma^2)^{1/2}$, ψ is the nucleon isospin doublet, $\vec{\pi}$ is the pseudoscalar-isovector pion field, σ is the scalar field, and ω_μ is a dynamically generated isoscalar vector field, which couples to the conserved baryonic current $j_\mu=\bar{\psi}\gamma_\mu\psi$. $\vec{\rho}_\mu$ is the isotriplet vector meson field with mass m_ρ. B and C are constant coefficients associated with the higher-order self-interactions of the scalar field.

The masses of the nucleon, scalar meson, and vector meson generated spontaneously by the Higgs mechanism are, respectively, given by

$$m=g_\sigma x_0,\quad m_\sigma=\sqrt{2\lambda}x_0,\quad m_\omega=g_\omega x_0. \tag{2}$$

Here x_0 is the vacuum expectation value of the σ field; g_ω, g_ρ, and g_σ are the coupling constants for the vector and scalar fields, respectively, and $\lambda=(m_\sigma^2-m_\pi^2)/(2f_\pi^2)$, where m_π is the pion mass and f_π is the pion decay coupling constant.

Using mean-field approximation, the equation of motion for the isoscalar vector meson field is

$$\omega_0=\frac{n_B}{g_\omega x^2}, \tag{3}$$

and that for the ρ field is given by

$$\rho_0^3=(g_\rho/2m_\rho^2)(n_p-n_n). \tag{4}$$

$n_B(=n_p+n_n)$ is the baryon number density at temperature T and is given by

$$n_B=\frac{\gamma}{(2\pi)^3}\int_0^\infty d^3k[n_i(T)-\bar{n_i}(T)], \tag{5}$$

with

$$n_i(T)=\frac{1}{e^{(E^*(k)-\nu_i)\beta}+1}, \tag{6}$$

$$\bar{n_i}(T)=\frac{1}{e^{(E^*(k)+\nu_i)\beta}+1}, \tag{7}$$

where $i=n,p$, $E^*(k)=(k^2+y^2m^2)^{1/2}$ is the effective nucleon energy, $\beta=1/K_BT$, and $\gamma(=2)$ is the spin degeneracy factor with $n_i(T)$ and $\bar{n_i}(T)$ being Fermi-Dirac distribution functions for particle and antiparticle, respectively, at finite temperature. ν_i is the effective baryon chemical potential which is related to the chemical potential μ_i as

$$\nu_p=\mu_p-\frac{C_\omega n_B}{y^2}-\frac{C_\rho}{4}(n_p-n_n), \tag{8}$$

$$\nu_n=\mu_n-\frac{C_\omega n_B}{y^2}+\frac{C_\rho}{4}(n_p-n_n). \tag{9}$$

The effective mass factor $y\equiv x/x_0$ must be determined self-consistently from the equation of motion for the scalar field which is given by

$$\begin{aligned} & (1-y^2)-\frac{B}{m^2C_\omega}(1-y^2)^2+\frac{C}{m^4C_\omega^2}(1-y^2)^3+\frac{2C_\sigma C_\omega n_B^2}{m^2y^4} \\ & -\frac{C_\sigma\gamma}{\pi^2}\int_0^\infty\frac{dkk^2(n_i(T)+\bar{n_i}(T))}{\sqrt{k^2+m^{*2}}}=0. \end{aligned} \tag{10}$$

$m^*\equiv ym$ is the effective mass of the nucleon and the coupling constants are expressed through

$$C_\sigma\equiv\frac{g_\sigma^2}{m_\sigma^2},\quad C_\omega\equiv\frac{g_\omega^2}{m_\omega^2},\quad \text{and } C_\rho\equiv g_\rho^2/m_\rho^2. \tag{11}$$

The symmetry energy coefficient that follows from the semi-empirical nuclear mass formula is [9]

$$a_{\text{sym}}=\frac{C_\rho k_f^3}{12\pi^2}+\frac{k_f^2}{6\sqrt{k_f^2+m^{*2}}}.$$

Now the nucleon number densities, energy density, and pressure at finite temperature and finite density are given by

$$n_p=\frac{\gamma}{(2\pi)^3}\int_0^\infty d^3k[n_p(T)-\bar{n_p}(T)], \tag{12}$$

$$n_n = \frac{\gamma}{(2\pi)^3}\int_0^\infty d^3k[n_n(T) - \overline{n_n}(T)], \tag{13}$$

$$\epsilon = \frac{m^2(1-y^2)^2}{8C_\sigma} - \frac{B}{12C_\omega C_\sigma}(1-y^2)^3 + \frac{C}{16m^2C_\omega^2C_\sigma}(1-y^2)^4 + \frac{C_\omega n_B^2}{2y^2} + \frac{1}{2}m_\rho^2(\rho_0^3)^2 + \frac{\gamma}{2\pi^2}\int_0^\infty dkk^2\sqrt{(k^2+m^{*2})} \times[n_n(T) + \overline{n_n}(T) + n_p(T) + \overline{n_p}(T)], \tag{14}$$

$$P = -\frac{m^2(1-y^2)^2}{8C_\sigma} + \frac{B}{12C_\omega C_\sigma}(1-y^2)^3 - \frac{C}{16m^2C_\omega^2C_\sigma}(1-y^2)^4 + \frac{C_\omega n_B^2}{2y^2} + \frac{1}{2}m_\rho^2(\rho_0^3)^2 + \frac{\gamma}{6\pi^2} \times \int_0^\infty \frac{dkk^4[n_n(T) + \overline{n_n}(T) + n_p(T) + \overline{n_p}(T)]}{\sqrt{(k^2+m^{*2})}}. \tag{15}$$

The entropy density (S/V) and entropy per baryon (S) can be obtained as

$$S/V = (P + \epsilon - \mu_p n_p - \mu_n n_n)\beta,$$

$$S = (P + \epsilon - \mu_p n_p - \mu_n n_n)\beta/n_B. \tag{16}$$

In order to describe the asymmetric nuclear matter one can introduce the proton fraction which is defined as

$$y_p = \frac{n_p}{n_B}, \tag{17}$$

for the neutron matter $y_p=0$ and for symmetric nuclear matter $y_p=0.5$.

The values of four parameters $C_\sigma, C_\omega, C_\rho, B$ and C occurring in the above equations are obtained [9] by fitting with the saturation values of binding energy/nucleon (-16.3 MeV), saturation density (0.153 fm^{-3}), symmetry energy (32 MeV), effective (Landau) mass (0.85 m), and nuclear incompressibility ($\sim$300 MeV), are $C_\omega=1.999$ fm^2, $C_\sigma=6.816$ fm^2, $C_\rho=4.661$ fm^2, $B=-99.985$, and $C=-132.246$. For a given value of n_B at fixed y_p and/or T, the equations [10,12,13] can be solved self-consistently to get y, μ_p, and μ_n, and using these values the energy density, pressure, entropy density, and entropy per baryon can be evaluated.

Now let us discuss the liquid-gas phase transition. In the case of the more common single component phase equilibria, such as liquid vapor, the phases are distinguished by only one parameter, e.g., the density, whereas the binary mixture has the additional parameter, the proton fraction y_p, which is different from one phase to another [22]. For the description of the liquid-gas phase transition we have followed here the thermodynamic approach of Refs. [16,22,23]. In the case of asymmetric nuclear matter, the system is characterized by two conserved charges, namely, the baryon density ($n_B=n_p+n_n$) and the total charge or equivalently the third component of isospin [$I_3=(n_p-n_n/2)$] or equivalently the proton fraction (y_p). Thus the stability criteria may be expressed by the following relations [16]:

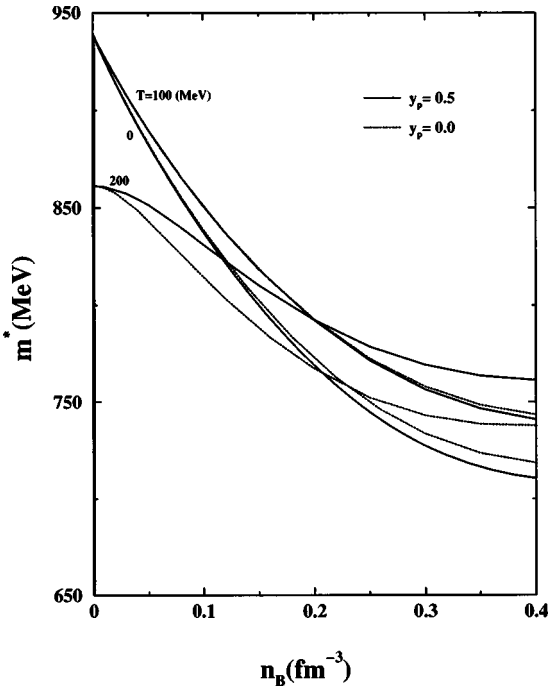

FIG. 1. Effective mass as a function of baryon number density at different temperatures.

$$n_B = \left(\frac{\partial P}{\partial n_B}\right)_{T,y_p} > 0, \tag{18}$$

$$\left(\frac{\partial \mu_p}{\partial y_p}\right)_{T,P} > 0, \text{ or } \left(\frac{\partial \mu_n}{\partial y_p}\right)_{T,P} < 0. \tag{19}$$

The first inequality shows that isothermal compressibility is positive which implies that the system is mechanically stable. The second condition expresses the diffusive stability. If any of the three stability criteria are violated then there will be a phase separation [7].

B. Results and discussions

First, we discuss the effective nucleon mass of nuclear matter at finite temperature and density. Figure 1 shows the effective mass versus number density at temperatures $T=0$, 100, and 200 MeV. The solid lines are for $y_p=0.5$ and the dotted lines are for $y_p=0$. It is observed that in all temperatures m^* decreases with the increase of n_B. For $T=0$ or $T=100$ MeV, the effective mass varies little with y_p, whereas it is very sensitive with y_p for $T=200$ MeV. It is also clear that at zero density, the effective mass is the same for neutron matter and symmetric matter at different temperatures. Hence, these results indicate [15] that the nucleons of neutron matter must stay in higher-energy levels compared to that of symmetric matter in order to have the same number density and the difference will decrease as the number density decreases. Further, the departure of m^* from its bare

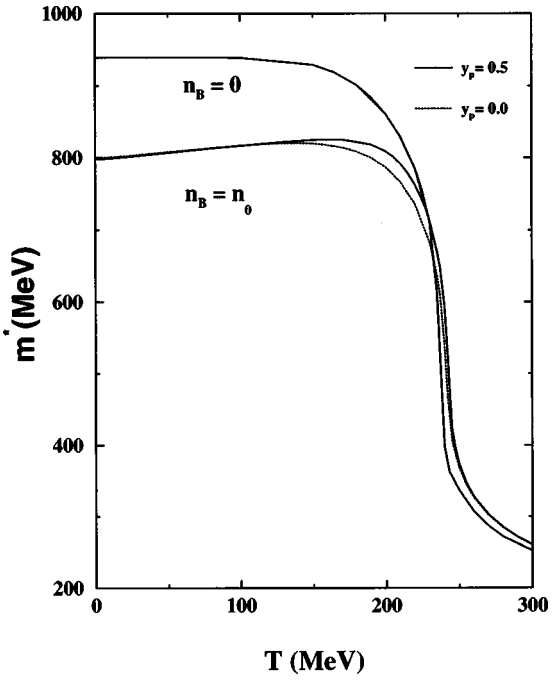

FIG. 2. Effective mass as a function of temperature for constant baryon number densities.

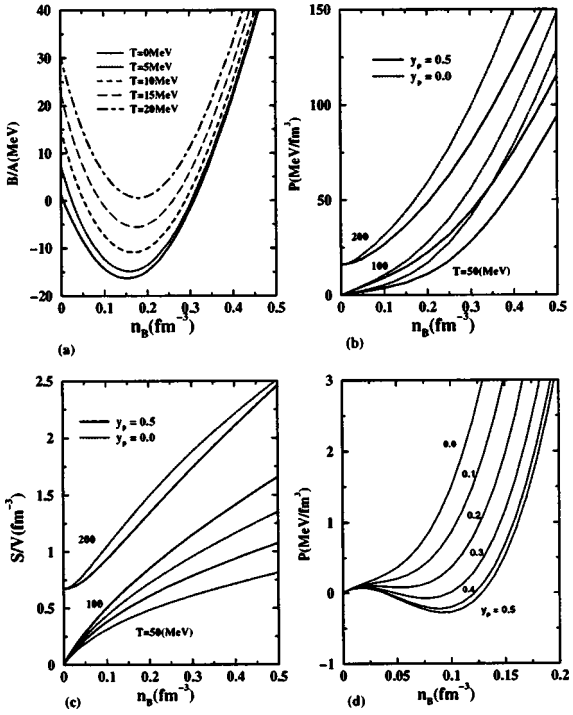

FIG. 3. (a) Binding energy per nucleon as a function of baryon number density at different temperatures for symmetric nuclear matter. (b) Pressure as a function of baryon number density at different temperatures. (c) Entropy density as a function of baryon number density at different temperatures. (d) Pressure as a function of baryon number density for different proton fractions at temperature $T=10$ MeV.

value at higher temperature as presented here has also been observed [15,25,26] by investigators working in other models. The explanation behind such an observation is obscure to us.

In Figure 2 we show the effective mass as a function temperature at zero density ($n_B=0$) and saturation density ($n_B=0.153$ fm^{-3}). The solid lines are for symmetric nuclear matter ($y_p=0.5$) and the dotted lines for neutron matter ($y_p=0$). It is clear from Fig. 2 that for $n_B=0$, the solid and dotted lines are the same, whereas for $n_B=n_0$, the y_p dependence is sensitive to the temperature lying between 150 and 240 MeV. The two lines again coincide at higher temperatures. It is also observed that for $n_B=n_0$, the m^* first increases slowly and then falls suddenly at about $T\approx 240$ MeV. But for $n_B=0$, m^* remains almost constant as the temperature increases and falls suddenly at about $T\approx 235$ MeV. This sudden fall indicates a first-order phase transition appearing for $n_B=0$, at $T\approx 235$ MeV similar to the result obtained for the Walecka model, which has such a phase transition at $T\approx 185$ MeV [24]. This effect has also been observed by Wang [15] at $T\approx 200$ MeV and by Hua, Bo, and Di Toro [25] at $T\approx 160$ MeV. Hua, Bo, and Di Toro [25] argue that because of the strong attraction between the nucleons at high temperatures the nucleon-antinucleon pairs can be formed which may lead to an abrupt change in m^* taking place in the high temperature region. But the mechanism of this first-order phase transition is no-clear.

Figure 3(a) shows the binding energy per nucleon as a function of the baryon density at different temperatures for symmetric nuclear matter, $y_p=0.5$. At zero temperature it has a minimum at the nuclear saturation density n_0 which corresponds to a binding energy per nucleon of −16.3 MeV. With the increase of temperature the minimum shifts towards higher densities and for higher temperatures the minimum of the curve becomes positive. It is also observed that as the temperature increases, the nuclear matter becomes less bound and the saturation curves in the MCH model look flatter than those observed in the Walecka model [25,26]. This result implies that the nuclear matter EOS in the MCH model is softer than that obtained in the Walecka model.

In Fig. 3(b), we show the pressure as a function of density n_B at different temperatures. The solid lines are for symmetric nuclear matter and the dotted lines are for pure neutron matter that is stiffer at all temperatures. For a given n_B, the pressure has the usual trend of increasing with temperature [27]. As the temperature increases the EOS becomes stiffer. The pressure has a nonzero value for $n_B=0$ at and above a temperature of 200 MeV. It indicates that the pressure has a contribution arising from the thermal distribution functions for baryons and antibaryons as well as from the nonzero value of the scalar field. Similar results were also obtained by Panda *et al.* [28] for symmetric nuclear matter. The nonzero value for scalar a field has also been observed in the Walecka model [27].

The entropy density as a function of density at different temperatures for symmetric nuclear matter and pure neutron matter is presented in Fig. 3(c). It is observed that the entropy density for both is nonzero even at a vanishing baryon density at a temperature of 200 MeV with contributions from the nonzero value of the sigma field. Similar behavior was also observed for the entropy density in the Walecka model and Zimanyi-Moszokowski (ZM) model calculations [26].

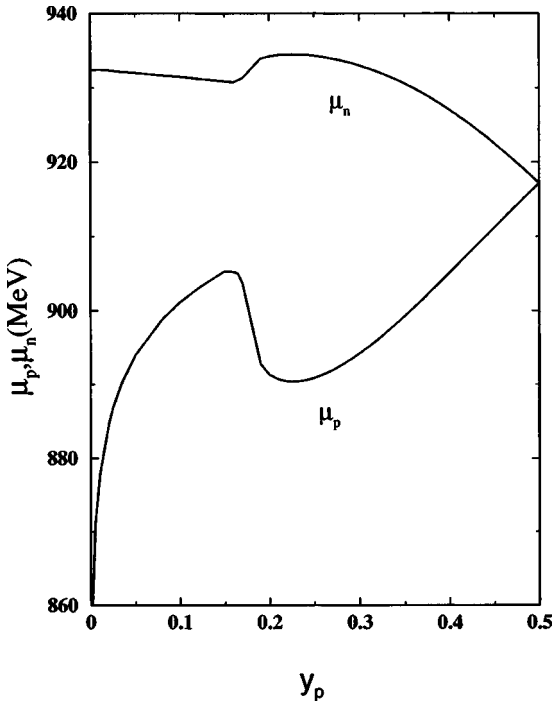

FIG. 4. Chemical potentials as a function of y_p at temperature $T=10$ MeV and $P=0.1$ MeV/fm^3.

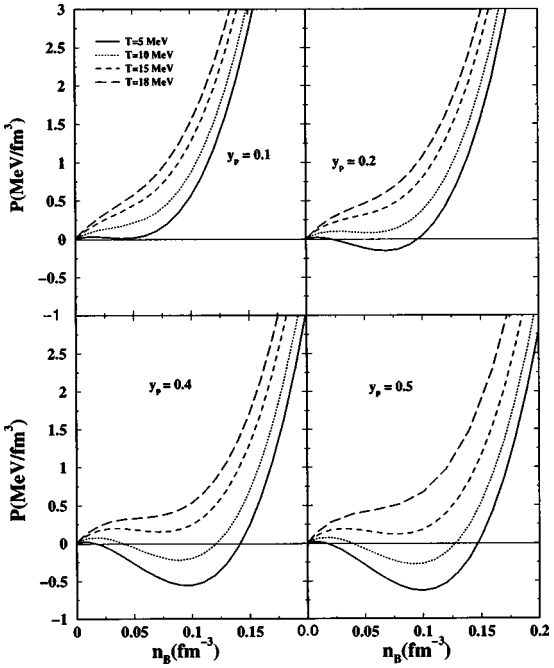

FIG. 5. Pressure as a function of baryon number density for different proton fractions.

This increase of entropy density with increase of temperature indicates a phase transition.

We now discuss the liquid-gas phase transition. The pressure as a function of baryon density at fixed temperature $T=10$ MeV with different proton fractions is shown in Fig. 3(d). It may be observed from Fig. 3(d) that for any fixed density with fixed $T=10$ MeV, the pressure is not constant, rather it increases with decrease of the proton fraction. This clearly indicates that for asymmetric nuclear matter during the isotherm liquid-gas phase transition the pressure cannot remain constant but increases monotonically. It shows that for small y_p, particularly for neutron matter ($y_p=0$), the pressure increases monotonically which indicates that matter is stable at all densities. But for $y_p \geqslant 0.2$, the compressibility becomes negative, indicating mechanical instability. The diffusive unstable regions can be seen clearly from Fig. 4, where the chemical potentials of proton and neutron are shown as a function of y_p at fixed pressure $P=0.1$ MeV/fm^3 and temperature $T=10$ MeV. According to the inequality [20] the region of negative slope for μ_p and positive slope for μ_n is unstable. Thus violation of stability criteria is an indication of phase separation.

Figure 5 shows the variation of pressure as a function of baryon density for different y_p. One can see that the region of mechanical instability decreases both with an increase of temperature and decrease of proton fraction [17]. Figure 5 shows that at zero temperature, the pressure first decreases, then increases and passes through P at $n_B=n_0$ (saturation density), where the binding energy per nucleon is a minimum. Decrease of pressure with density implies a negative incompressibility, $K=9(\partial P/\partial n_B)$, which is a sign of mechanical instability. When the temperature increases the region of mechanical instability decreases and disappears at the critical temperature T_c, which is determined by $\partial P/\partial n_B|_{T_c} = \partial^2 P/\partial^2 n_B|_{T_c}=0$, above which the liquid-gas phase transition is continuous. For $y_p=0.5$, we have obtained the value of critical temperature $T_c \approx 17.2$ MeV, critical density $n_c \approx 0.045$ fm^{-3}, critical pressure $p_c \approx 0.274$ MeV/fm^{-3}, and critical effective mass $m_c^* \approx 887$ MeV, which is in fair agreement with the results obtained in other studies [17,25,26].

In Fig. 6, we plot the variation of critical temperature with different proton fractions (y_p) with and without ρ. The critical temperature T_c decreases monotonically [17,29] as the proton fraction decreases and goes to zero for $y_p=0.02$ with

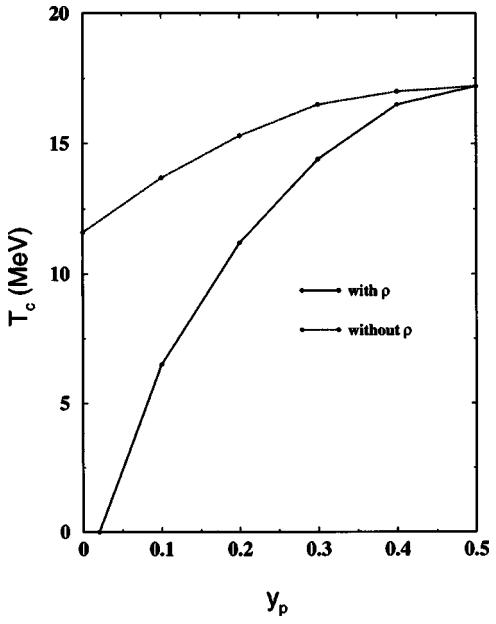

FIG. 6. Critical temperature vs proton fraction y_p.

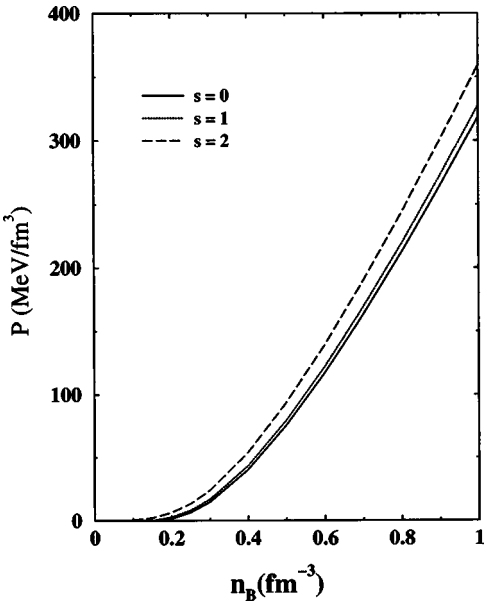

FIG. 7. Pressure as a function of number density at fixed entropy per baryon.

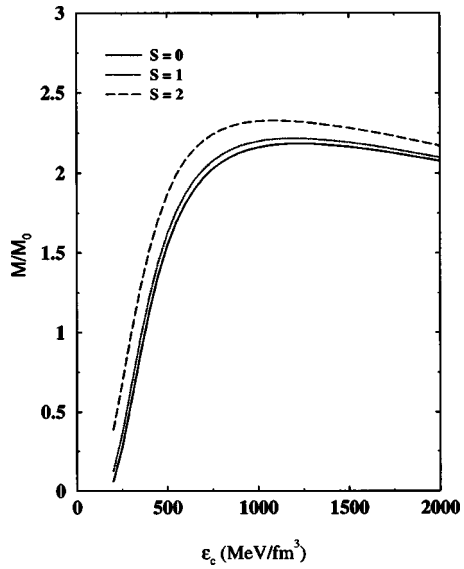

FIG. 8. Star mass ($M/M_\odot$) as a function of central energy density at fixed entropy per baryon.

ρ, whereas $T_c = 11.6$ at $y_p = 0$ without ρ. This indicates that addition of the ρ meson lowers the critical temperature at smaller y_p. As may be seen from the equations [8,9], the addition of the ρ meson gives a repulsive potential which makes the nuclear matter easier to be gasified. But for neutron matter ($y_p = 0$), the system only remains in the gas phase even at zero temperature [15].

III. PROTO-NEUTRON STAR

In this section, as our second application, we undertake a study of the structure and properties of the proto-neutron star. A PNS is born following the gravitational collapse of the core of a massive star during a supernova explosion (type II). It is a hot collapsed core which can reach temperatures as high as few tens of MeV. The evolution of the PNS proceeding through several distinct states with various outcomes is discussed in Ref. [11]. During the early evolution of the PNS, a neutron star with an entropy per baryon of order of unity contains neutrinos that are trapped in matter on a dynamical time scale and after a lapse of a few tens of seconds the star achieves its cold catalyzed structure with essentially zero temperature and zero trapped neutrinos. A PNS has approximately uniform entropy per baryon (S) of 1-2 across the star [30]. At birth the PNS has $S = 1$. After deleptonization the entropy per baryon reaches its maximum ($S \sim 2$) and finally cools down to its cold state with $S = 0$ [11]. The finite temperature aspect of the EOS plays an important role in the study of the properties and structure of the PNS.

The structure of the PNS mainly depends on its composition [11]. Since the composition of the neutron star basically depends on the nature of the strong interactions, which are not well understood in dense matter, one has to investigate various possible conditions taking many possible models. Out of the various possible cases discussed in Ref. [11], we consider here a case in which matter consists of neutrons, protons, and electrons whose relative concentrations are determined from the conditions of charge neutrality and β equilibrium in the absence of neutrino trapping [11].

The β equilibrium (without neutrino trapping) and the charge neutrality conditions are, respectively, given by

$$\mu_n = \mu_p + \mu_e, \tag{20}$$

and

$$n_p = n_e, \tag{21}$$

where μ_e and n_e are the chemical potentials and number density of electrons, respectively.

The electron number density at finite temperature can be written as

$$n_e = \frac{\gamma}{(2\pi)^3}\int_0^\infty d^3k[n_e(T) - \overline{n_e}(T)], \tag{22}$$

where

$$n_e(T) = \frac{1}{e^{(\sqrt{(k^2+m_e^2)}-\mu_e)\beta}+1}, \quad \overline{n_e}(T) = \frac{1}{e^{(\sqrt{(k^2+m_e^2)}+\mu_e)\beta}+1}. \tag{23}$$

The number density of neutrons and protons is defined in Eqs. (12) and (13). The extra terms which must be added to the energy density and pressure [given in Eqs. (14) and (15)] are, respectively,

$$\frac{\gamma}{2\pi^2}\int_0^\infty dk k^2\sqrt{(k^2+m_e^2)}[n_e(T) + \overline{n_e}(T)], \tag{24}$$

and

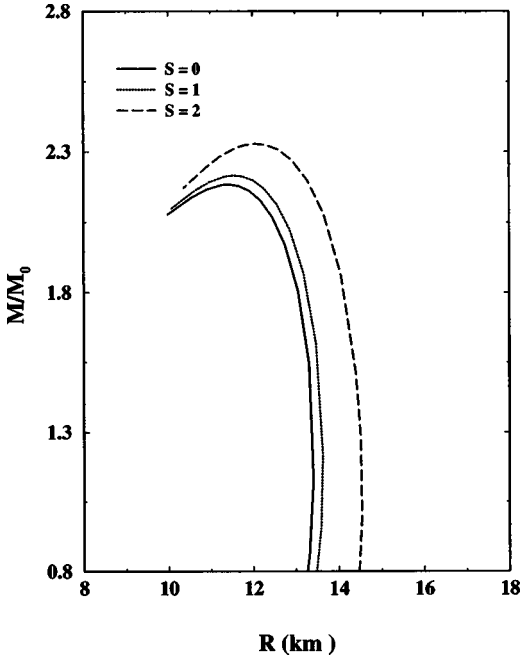

FIG. 9. Radius vs star mass at fixed entropy per baryon.

$$\frac{\gamma}{6\pi^2}\int_0^\infty \frac{dkk^4[n_e(T)+\overline{n_e}(T)]}{\sqrt{(k^2+m_e)}}. \tag{25}$$

For a given value of n_B, with fixed $S=0,1$, or 2, the equations [10,12,13,16,22] are to be solved self-consistently using Eqs. (20) and (21) to get μ_p,μ_e,n_p,y, and T, and from which we get $\mu_n(=\mu_p+\mu_e)$ and $y_p(=n_p/n_B)$. Then these values can be substituted to get the pressure and energy density. After getting the pressure as a function of the energy density, the TOV equations can be integrated using the proper boundary conditions [9] to get the mass and radius of the star at fixed entropy per baryon S.

The pressure as a function of number density for $S=0,1$, and 2 is shown in Fig. 7. One can mark from Fig. 7 that the EOS becomes softer as the entropy per baryon decreases from $S=2$ to $S=0$, which indicates the lowering of mass and radius, as shown in Figs. 8 and 9, respectively. For different values of S, the radius, energy density, pressure, number density, and temperature corresponding to the maximum mass are given in Table I.

The results in Table I reflect the influence of entropy on the gross properties of stars. It is observed that an increase in maximum mass and radius up to $S=2$ amounts to only a few percent of their respective values for the cold star, and the maximum temperature of the core is found to be around

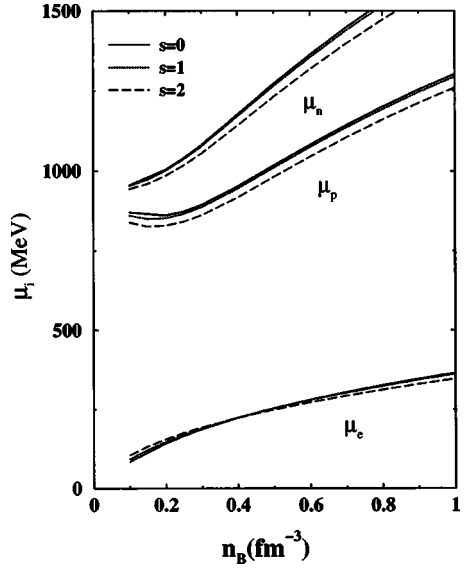

FIG. 10. Chemical potential vs number density in beta equilibrium at fixed entropy per baryon S.

62 MeV, which is in fair agreement with the results obtained in Ref. [11]. In neutron stars, the pressure is supported, largely provided by strongly interacting baryons which have relatively smaller thermal contributions to the pressure. This results in a small increase in the maximum mass of the neutron star. Thus the compositional variable of EOS plays a more important role than the temperature for the structure of neutron star [11].

The chemical potentials of n,p, and e in beta equilibrium for fixed entropy per baryon $S=0,1$, and 2 are shown in Fig. 10. It is clear that μ_e increases linearly with number density whereas μ_n and μ_p first decrease and then increase linearly. The increase of electron chemical potential with number density implies the abundance of negatively charged particles (electrons) which shows that the system has a large number of protons over an extended region of density. It may be seen from Fig. 10 that in the very lower-density region the proton abundance is large, then decreases to some extent, and then increases linearly in the high-density region.

The temperature as a function of energy density at fixed entropy per baryon is shown in Fig. 11. The temperature of the star increases for both $S=1$ and $S=2$ from which one can get the critical temperature corresponding to the maximum mass of the star. The temperature is maximum at the center of the star (where the central energy density is about $1100-1200$ MeV/fm^3 for a maximum mass star) and decreases with decreasing energy density, which is faster particularly at lower energy densities. This implies that the in-

TABLE I. Star properties for matter in beta equilibrium at finite entropy.

S	$M_{\max}/M_\odot$	R (km)	ϵ_c (MeV/fm^3)	n_c (fm^{-3})	P_c (MeV/fm^3)	T_c (MeV)
0	2.18	12.14	1230	0.97	304.71	0.0
1	2.21	12.23	1190	0.94	294.85	27.85
2	2.33	12.45	1092	0.85	272.24	62.12

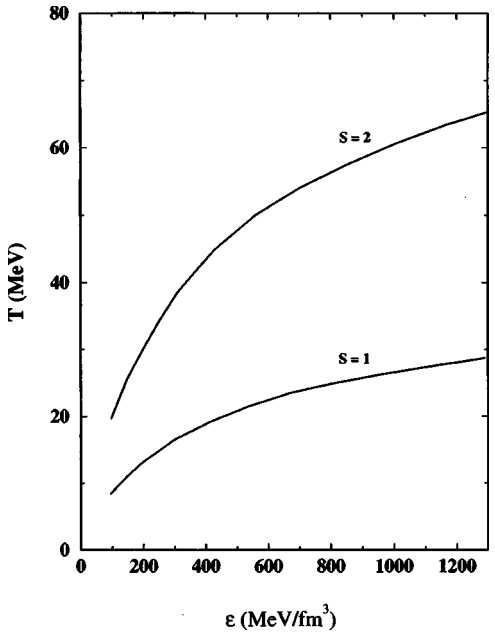

FIG. 11. Temperature vs energy density of the proto-neutron star.

terior of the star maintains a small variation of temperature but falls rapidly towards the surface region as the density decreases.

IV. CONCLUSIONS

We, in this work, have applied the MCH model [9] to the study of asymmetric nuclear matter at finite temperature and the structure of a PNS. We have presented the behavior of the effective nucleon mass, energy per baryon, entropy density, entropy per baryon, and pressure as a function of density of asymmetric nuclear matter for various temperatures. At zero density we find that this model exhibits a phase transition at $T \approx 235$ MeV just as obatined in the Walecka model at $T \approx 185$ MeV. This model exhibits the existence of a liquid-gas phase transition in asymmetric nuclear matter and the critical temperature T_c depends sensitively on the proton fraction y_p. T_c decreases with the decrease of y_p as shown in Fig. 6. The value of the critical temperature decreases from $T_c \approx 17.2$ to 11.6 MeV for $y_p = 0.5$ to 0 without the ρ meson and from $T_c \approx 17.2$ to 0 MeV for $y_p = 0.5$ to 0.2 with the ρ meson. Hence, the addition of the ρ meson seems to be very important to the study of the properties of asymmetric nuclear matter as it lowers the critical temperature. This also shows that even at zero temperature the system remains only in the gas phase for neutron matter ($y_p = 0$). At fixed temperature and density the pressure of the system increases with the decrease of the proton fraction [shown in Fig. 3(d)], which indicates that during the isotherm liquid-gas phase transition the pressure cannot remain constant for asymmetric nuclear matter. In comparision with other models T_c varies with y_p in all models but the values are different in different mean-field models such as at $y_p = 0.5$, T_c varies as 18.3 MeV [18], 12.66 MeV [25], 14.30 MeV [15], 16.50 MeV [26], and 15.75 MeV [16].

We have also studied the EOS and structure of a PNS with neutrino free charge neutral matter in beta equilibrium. We find that as the PNS cools from $S = 2$ to $S = 0$, the maximum mass and radius exhibit a slow decrease. Thus the influence of entropy per baryon, or equivalently the temperature on the structure of PNS, is not very sensitive. It is also observed that at finite entropy per baryon, the star has a large number of protons over an extended region of density. The temperature varies slowly in the interior of the star but falls rapidly towards the low density surface region and the maximum temperature of the core of the star for $S = 2$ is about 62 MeV. All these results of the PNS are in fair agreement with that obtained in Ref. [11].

ACKNOWLEDGMENTS

P. K. Jena would like to thank the Council of Scientific and Industrial Research, Government of India, for the award of SRF, with financial support under Grant No. 9/173 (101)/2000/EMR-I. Help of the Institute of Physics, Bhubaneswar, India, is warmly acknowledged for providing the library and computational facility.

[1] J. D. Walecka, Ann. Phys. (N.Y.) **83**, 491 (1974).
[2] S. A. Chin, Ann. Phys. (N.Y.) **108**, 301 (1977); B. D. Serot, Phys. Lett. **86B**, 146 (1979); C. J. Horowitz and B. D. Serot, Nucl. Phys. **A368**, 503 (1981); J. Boguta and A. R. Bodmer, *ibid.* **A292**, 413 (1977).
[3] T. D. Lee and G. C. Wick, Phys. Rev. D **9**, 2291 (1974).
[4] A. D. Jackson and M. Rho, Nucl. Phys. **A407**, 495 (1985).
[5] J. Boguta, Phys. Lett. **120B**, 34 (1983); **128**, 19 (1983).
[6] P. K. Sahu, R. Basu, and B. Datta, Astrophys. J. **416**, 267 (1993).
[7] N. K. Glendenning, Nucl. Phys. **A480**, 597 (1988).
[8] P. K. Sahu and A. Ohnishi, Prog. Theor. Phys. **104**, 1163 (2000).
[9] P. K. Jena and L. P. Singh, Mod. Phys. Lett. A **17**, 2633 (2002); **18**, 2135 (2003).
[10] E. Baron, J. Cooperstein, and S. Kahana, Phys. Rev. Lett. **55**, 126 (1985); M. Brak, C. Guet, and H. B. Hakansson, Phys. Rep. **123**, 277 (1985).
[11] M. Prakash, I. Bombaci, M. Prakash, P. J. Ellis, J. M. Lattimer, and R. Knorren, Phys. Rep. **280**, 1 (1997).
[12] W. A. Kupper, G. Wegmann, and E. R. Hilf, Ann. Phys. (N.Y.) **88**, 454 (1974); B. Freedman and V. R. Pandharipande, Nucl. Phys. **A361**, 502 (1981); H. Jaqaman, A. Z. Mekjian, and L. Zamick, Phys. Rev. C **27**, 2782 (1983); D. Bandyopadyay, C. Samanta, S. K. Samaddar, and J. N. De, Nucl. Phys. **A511**, 1 (1990).
[13] H. Q. Song, Z. X. Qian, and R. K. Su, Phys. Rev. C **47**, 2001 (1993).

[14] H. Q. Song and R. K. Su, Phys. Lett. B **355**, 179 (1995).
[15] P. Wang, Phys. Rev. C **61**, 054904 (2003).
[16] H. Müller and B. D. Serot, Phys. Rev. C **52**, 2072 (1995).
[17] P. K. Panda, G. Krein, D. P. Menezes, and C. Providencia, Phys. Rev. C **68**, 015201 (2003).
[18] B. D. Serot and J. D. Walecka, Adv. Nucl. Phys. **16**, 1 (1986); B. D. Serot, Int. J. Mod. Phys. E **6**, 515 (1997).
[19] J. A. Pons, S. Reddy, M. Prakash, J. M. Lattimer, and J. A. Miralles, Astrophys. J. **513**, 780 (1999).
[20] G. F. Marranghello, C. A. Z. Vasconcellos, M. Dillig, and J. A. D. F. Pacheco, Int. J. Mod. Phys. E **11**, 83 (2002).
[21] P. K. Jena and L. P. Singh, nucl-th/0306085.
[22] M. Barranco and J. R. Buchler, Phys. Rev. C **22**, 1729 (1980).
[23] N. K. Glendenning, Phys. Rev. D **46**, 1274 (1992).
[24] J. Theis, G. Graebner, G. Buchwald, J. Maruhn, W. Greiner, H. Stöcker, and J. Polonyi, Phys. Rev. D **28**, 2286 (1983).
[25] Guo Hua, Liu Bo, and M. Di Toro, Phys. Rev. C **62**, 035203 (2000).
[26] M. Malheiro, A. Delfino, and C. T. Coelho, Phys. Rev. C **58**, 426 (1998).
[27] R. J. Furnstahl and B. D. Serot, Phys. Rev. C **41**, 262 (1990).
[28] P. K. Panda, A. Mishra, J. M. Eisenberg, and W. Greiner, Phys. Rev. C **56**, 3134 (1997).
[29] S. Ray, J. Shamanna, and T. T. S. Kuo, Phys. Lett. B **392**, 7 (1997).
[30] A. Burrows and J. M. Lattimer, Astrophys. J. **307**, 178 (1986).